

# Methylmercury photodegradation influenced by sea-ice cover in Arctic marine ecosystems

D. Point<sup>1,2\*</sup>, J. E. Sonke<sup>2</sup>, R. D. Day<sup>1</sup>, D. G. Roseneau<sup>3</sup>, K. A. Hobson<sup>4</sup>, S. S. Vander Pol<sup>1</sup>, A. J. Moors<sup>1</sup>, R. S. Pugh<sup>1</sup>, O. F. X. Donard<sup>5</sup> and P. R. Becker<sup>1</sup>

**Atmospheric deposition of mercury to remote areas has increased threefold since pre-industrial times. Mercury deposition is particularly pronounced in the Arctic. Following deposition to surface oceans and sea ice, mercury can be converted into methylmercury, a biologically accessible form of the toxin, which biomagnifies along the marine food chain. Mass-independent fractionation of mercury isotopes accompanies the photochemical breakdown of methylmercury to less bioavailable forms in surface waters. Here we examine the isotopic composition of mercury in seabird eggs collected from colonies in the North Pacific Ocean, the Bering Sea and the western Arctic Ocean, to determine geographical variations in methylmercury breakdown at northern latitudes. We find evidence for mass-independent fractionation of mercury isotopes. The degree of mass-independent fractionation declines with latitude. Foraging behaviour and geographic variations in mercury sources and solar radiation fluxes were unable to explain the latitudinal gradient. However, mass-independent fractionation was negatively correlated with sea-ice cover. We conclude that sea-ice cover impedes the photochemical breakdown of methylmercury in surface waters, and suggest that further loss of Arctic sea this century will accelerate sunlight-induced breakdown of methylmercury in northern surface waters.**

Mercury (Hg) deposition to remote environments has increased by a factor of  $3 \pm 1$  since pre-industrial times<sup>1</sup>. Mercury levels are often enhanced in northern marine wildlife species<sup>2–4</sup>, posing a health risk for the people who regularly consume these subsistence resources<sup>5</sup>. The view that the Arctic is a sink for Hg emerged with the discovery of atmospheric Hg depletion events that occur after polar sunrise<sup>6</sup>. Once deposited, a fraction of Hg is re-emitted back to the atmosphere<sup>7,8</sup> and a remaining fraction can be methylated to produce neurotoxic methylmercury<sup>9</sup> (MeHg). This organic form of Hg can be biomagnified and its concentration in top predators is influenced by ecological processes, including the length and structure of the food webs<sup>10,11</sup>. Whereas a cascade of processes might link global atmospheric Hg emissions to Hg concentrations in Arctic biota, the contrasting spatiotemporal trends that show an increase in Hg concentrations in biota in the Canadian Arctic west of Greenland and a decrease east of Greenland and around Iceland<sup>12</sup> cannot be explained solely by net atmospheric Hg deposition. Different Hg sources and/or climate change effects on Hg biogeochemistry and food web structures have been suggested as possible alternative factors underlying these trends<sup>7,13</sup>. Our incomplete understanding of the coupling that exists between the incorporation of Hg and its biomagnification in the food chain and its geochemical cycle has limited our ability to answer these questions.

Our present understanding of the global Hg cycle is based on the spatial and temporal variations in concentrations of chemical Hg species. Recent advances in mass spectrometry have allowed us to investigate natural variations in the stable isotopic composition of Hg and explore a new dimension of information on the

biological and physicochemical processes that relate Hg sources to sinks<sup>14</sup>. Virtually all chemical transformations involving Hg, such as photochemistry, abiotic and bacterial reduction, bacterial demethylation, abiotic oxidation, evaporation, condensation and human metabolism fractionate Hg isotopes as a function of isotope mass<sup>15–18</sup>. In addition, photochemical transformations of Hg compounds may induce Hg isotopic variations that are independent of isotope mass<sup>18,19</sup>, a rare phenomenon that has previously been observed in natural terrestrial processes only for the elements oxygen and sulphur<sup>20,21</sup>. Mass-independent fractionation (MIF) of MeHg and inorganic mercury (iHg) during aquatic photoreduction enriches the residual Hg pool in the odd Hg isotopes<sup>18</sup>, whereas the evading Hg<sup>0</sup> gas becomes depleted in the odd Hg isotopes<sup>14</sup>. Hg MIF signatures in natural samples were first observed as excess odd-isotope anomalies in freshwater fish and invertebrates<sup>18,22</sup>. Despite suggestions that bacterial Hg methylation or *in vivo* fish metabolism might cause MIF (refs. 22,23), experiments, field observations and theoretical considerations indicate that biochemical MIF is unlikely<sup>15,17,24</sup>. As a result, the uptake of residual aquatic iHg and MeHg after MIF-inducing photoreduction<sup>17,18</sup> remains the most plausible explanation for the biological MIF anomalies. This implies that the anomalies found in aquatic food webs provide direct windows into Hg MIF variations in aquatic ecosystems.

## Spatial variations in seabird egg Hg isotopic composition

We analysed cryogenically banked common murre (*Uria aalge*) and thick-billed murre (*Uria lomvia*) eggs from three geographic regions in Alaska (Fig. 1a) for mercury and nitrogen isotopes. Murres remain in the northern latitudes year-round and Alaskan

<sup>1</sup>National Institute of Standards and Technology (NIST), Hollings Marine Laboratory, Charleston, South Carolina 29412, USA, <sup>2</sup>Laboratoire des Mécanismes et Transferts en Géologie (LMTG), Observatoire Midi-Pyrénées, UMR CNRS 5563, UMR IRD 154, Université Paul Sabatier, 31400 Toulouse, France, <sup>3</sup>US Fish and Wildlife Service, Alaska Maritime National Wildlife Refuge, Homer, Alaska 99603, USA, <sup>4</sup>Environment Canada, Saskatoon, Saskatchewan, S7N 0X4, Canada, <sup>5</sup>Institut Pluridisciplinaire de Recherche sur l'Environnement et les Matériaux, Equipe de Chimie Analytique BioInorganique et Environnement, UMR CNRS 5254, 64053 Pau, France. \*e-mail: david.point@lmtg.obs-mip.fr.

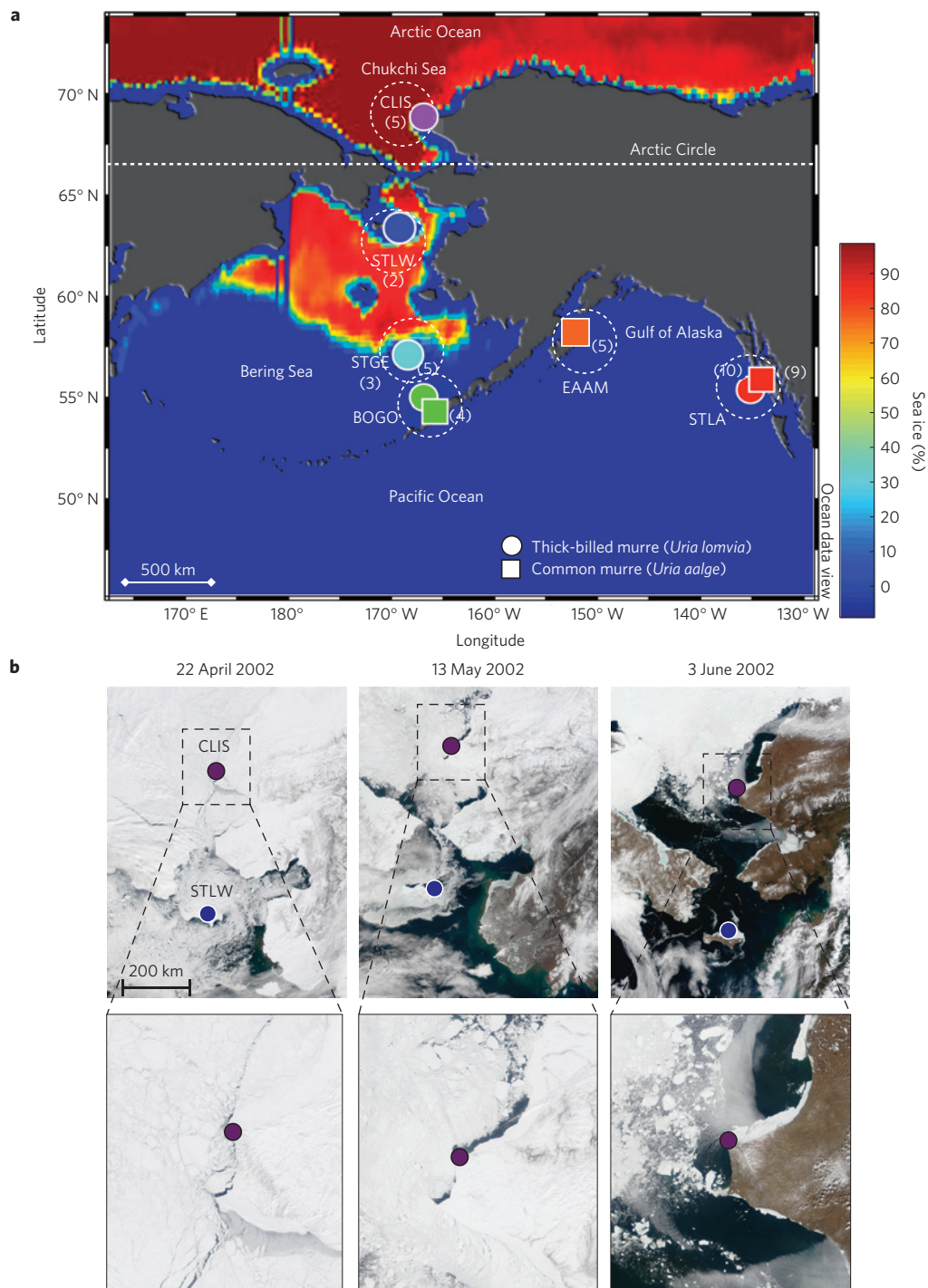


**Figure 1 | Common and thick-billed murre colony locations and sea-ice conditions at the beginning of the 2002 breeding season. a**, The colonies include Cape Lisburne (CLIS) in the Chukchi Sea; St Lawrence (STLW), St George (STGE) and Bogoslof islands (BOGO) in the Bering Sea; and East Amatuli (EAAM) and St Lazaria islands (STLA) in the Gulf of Alaska (see Supplementary Table S1). Numbers of samples analysed from the colonies are shown in parentheses, and the dashed circles show the maximum 170 km foraging range around them. Sea-ice concentrations (%) show the relative amounts of ice in 25 km by 25 km blocks in late March 2002. **b**, Murres breeding at northern latitudes stage and forage in the open lead systems shown in the inset pictures.

birds winter in the Bering Sea and Gulf of Alaska<sup>25–27</sup>. Gulf of Alaska murre colonies usually winter along the gulf's shelf break and in bays and inlets of this region, and begin returning to the region's nesting colonies up to six to eight weeks before they lay eggs<sup>28,29</sup>. Most of the murre colonies nesting in the northern Bering and eastern Chukchi seas winter in and near the southern Bering sea-ice front and also return to their respective northern breeding locations well before they

lay eggs<sup>27</sup>. When these birds arrive, the waters near their colonies are still covered by ice, and as a result, they stage and forage in the open lead systems (Fig. 1b) for several weeks. Murres lay large single eggs that have been identified as key tissues for monitoring contaminants, particularly Hg, in northern latitudes<sup>30–32</sup>. Egg Hg contents (essentially MeHg; refs 31,33) reflect the female's dietary exposure during egg formation<sup>34</sup>.

The even-mass isotopes 198, 200 and 202 exhibited mass-dependent fractionation (MDF) in the egg samples, as illustrated in a  $\delta^{200}\text{Hg}$  versus  $\delta^{202}\text{Hg}$  isotope diagram (Fig. 2a). Odd-mass isotopes  $^{199}\text{Hg}$  and  $^{201}\text{Hg}$ , diagrammed for  $\delta^{201}\text{Hg}$  versus  $\delta^{202}\text{Hg}$  in Fig. 2b (see Supplementary Fig. S1a for  $\delta^{199}\text{Hg}$ ), show MIF in all the samples. The observed deviation from the MDF line, as expressed in  $\Delta^{201}\text{Hg}$  notation<sup>35</sup> (Fig. 2c, see Supplementary Fig. S1b for  $\Delta^{199}\text{Hg}$ ) shows that paired  $\delta^{202}\text{Hg}$  and  $\Delta^{201}\text{Hg}$  clearly separate murre geographically. Noticeably lower average MIF values were found above the Arctic Circle in the eastern Chukchi Sea ( $\Delta^{201}\text{Hg}$  of  $+0.48\text{‰} \pm 0.08\text{‰}$ ; mean  $\pm$  s.d.,  $n = 5$ ), compared with the southern Bering Sea and Gulf of Alaska ( $\Delta^{201}\text{Hg}$  of  $+0.92\text{‰} \pm 0.12\text{‰}$ ; mean  $\pm$  s.d.,  $n = 12$ , and  $+1.00\text{‰} \pm 0.09\text{‰}$ ; mean  $\pm$  s.d.,  $n = 24$ , respectively). Murres are capable of foraging as far as 170 km from their nesting colonies<sup>36</sup>, but our study sites were separated by distances that were greater than this, with the exception of St George and Bogoslof islands (Fig. 1a). This is a strong indication that the trends and differences found in MeHg isotopic composition in the murre eggs did not result from overlaps in foraging areas, but were more likely related to other factors, including ecological and biogeochemical processes and/or differences in mercury sources.

### Role of seabird foraging ecology and climate

Murre diets traced by  $\delta^{15}\text{N}$ , and converted to trophic level by normalizing for geographical  $\delta^{15}\text{N}$  baselines (see Supplementary Method S1), clearly indicate differences in foraging behaviour among regions (Fig. 3). Murres nesting at colonies in the southern Bering Sea, where invertebrates play an important role in their diets<sup>37</sup>, occupied a lower trophic level than the Gulf of Alaska and Chukchi Sea birds, where fish are the primary prey<sup>38,39</sup>. These differences influence Hg exposure and transfer, especially at the more southern colonies, where trophic level noticeably influenced egg Hg concentrations (Fig. 3a). In contrast, the colonies as a whole showed a weaker, but still noticeable trend, because of lower Hg levels in the eggs of birds nesting at more northern latitudes, particularly birds nesting in the eastern Chukchi Sea (Cape Lisburne). This may reflect differences in Hg concentrations in the local food webs or differences in food web structure.

Hg MDF (Fig. 3b) seemed to be particularly sensitive to ecological effects, with  $\delta^{202}\text{Hg}$  increasing overall by  $1.36\text{‰} \pm 0.35\text{‰}$  (s.e.m.) per trophic level for all colonies ( $1.56\text{‰} \pm 0.28\text{‰}$  (s.e.m.) for colonies at more southern latitudes), similar to the findings of other published food web studies<sup>17,22</sup>. Conversely, Hg MIF parameters did not seem to be influenced by foraging behaviour at the more southern latitudes, or among the colonies as a whole (Fig. 3c). This indicates there is a low probability of *in vivo* biochemical MIF during Hg trophic transfer and metabolism events<sup>15,17</sup>. Moreover, egg Hg MIF tends to decrease with increasing latitude (Fig. 4 and Supplementary Table S1:  $\Delta^{201}\text{Hg}$  (and  $\Delta^{199}\text{Hg}$ ) decreased by  $0.43\text{‰}$  between  $54^\circ$  and  $69^\circ$  north). Murres nesting at northern latitudes at the eastern Chukchi Sea and northern and southern Bering Sea colonies overwinter in the same general region of the southern Bering Sea<sup>27</sup>. Therefore, the lower egg Hg MIF patterns found in the birds nesting at the northern colonies are probably acquired on their breeding grounds. This implies that northern and southern ecosystems have distinct Hg MIF ( $\Delta^{201}\text{Hg}$ ) signatures. At present, it is understood that the substantially positive MIF signatures ( $\Delta^{201}\text{Hg}$  reported up to  $5\text{‰}$ ; ref. 18) of marine and freshwater aquatic organisms are the result of surface water photochemical iHg and/or MeHg photoreduction, followed by uptake and bioaccumulation along the food chain<sup>14,17,18,40</sup>. Therefore it is likely that the latitudinal MIF gradient may be geochemically controlled by surface ocean photochemistry conditions. However, the possibility must be considered that geographic variations in atmospheric source MIF signatures are responsible for the latitudinal MIF gradient. The atmospheric deposition of Hg in Alaskan marine environments

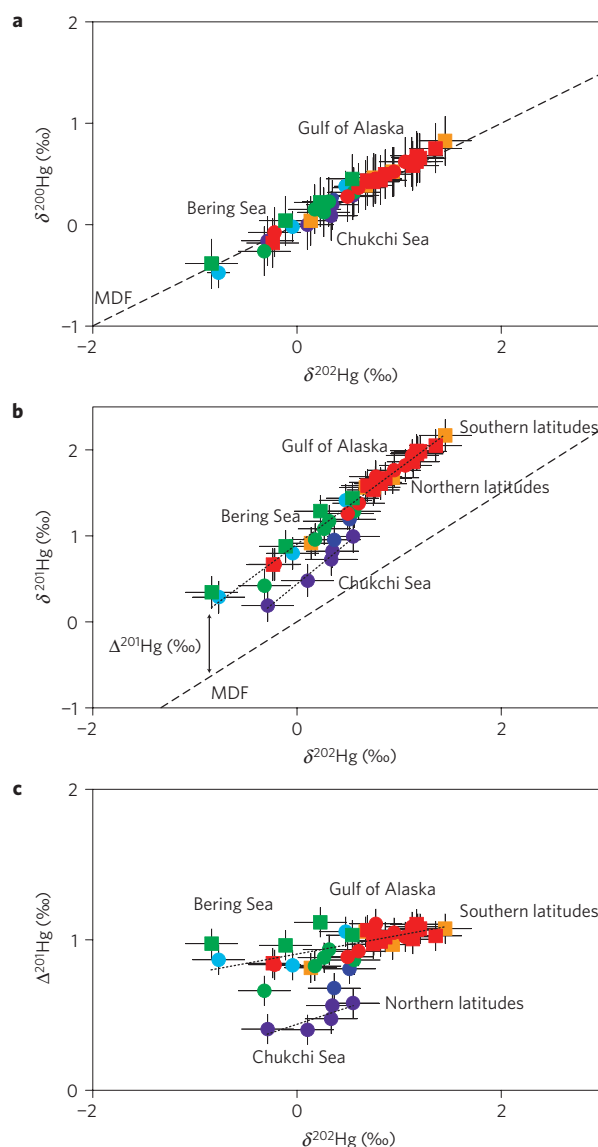


**Figure 2 | Mercury three-isotope diagrams illustrating variations in mercury MDF and MIF in murre eggs.** **a–c**,  $\delta^{202}\text{Hg}$  plotted against  $\delta^{200}\text{Hg}$  (**a**),  $\delta^{201}\text{Hg}$  (**b**) and  $\Delta^{201}\text{Hg}$  (**c**). See Fig. 1 for legend. The dashed lines in **a** and **b** represent the theoretically predicted MDF based on the  $\delta^{202}\text{Hg}$  values<sup>35</sup>. Mercury  $\delta^{199}\text{Hg}$  and  $\Delta^{199}\text{Hg}$  information is shown in Supplementary Fig. S1. The dotted lines in **b** and **c** show the regression trends for the birds breeding at northern latitudes (eastern Chukchi Sea) and southern latitudes (southern Bering Sea and Gulf of Alaska). The uncertainties reported for the samples are the external reproducibility ( $n = 7$ ) of the method used for NIST Murre Egg Control Material QC04-ERM1 ( $\pm 0.26\text{‰}$ ,  $2\sigma$ , s.d. for  $\delta^{202}\text{Hg}$ , and  $\pm 0.10\text{‰}$ ,  $2\sigma$ , s.d. for  $\Delta^{201}\text{Hg}$ ).

reflects well-mixed northern hemispheric Hg emissions. Asian emissions are estimated to represent up to 20% of Alaskan Hg deposition<sup>41</sup>. Alternatively, modelled contribution estimates of anthropogenic Hg contributions to North Pacific ocean dissolved Hg amount to only 9% (ref. 42). Regional variations in coal Hg MIF exist, for example  $\Delta^{201}\text{Hg}$  of  $0.04\text{‰} \pm 0.16\text{‰}$ ,  $-0.34\text{‰} \pm 0.19\text{‰}$  and  $-0.13\text{‰} \pm 0.12\text{‰}$  (mean  $\pm$  s.d.) for Chinese, Russian and North American coal, respectively<sup>43</sup>. However, in spite of these marked variations in coal  $\Delta^{201}\text{Hg}$ , any latitudinal variations in coal-related Hg deposition in northern environments seem too small in magnitude to explain the  $0.43\text{‰}$  gradient found in egg  $\Delta^{201}\text{Hg}$ .

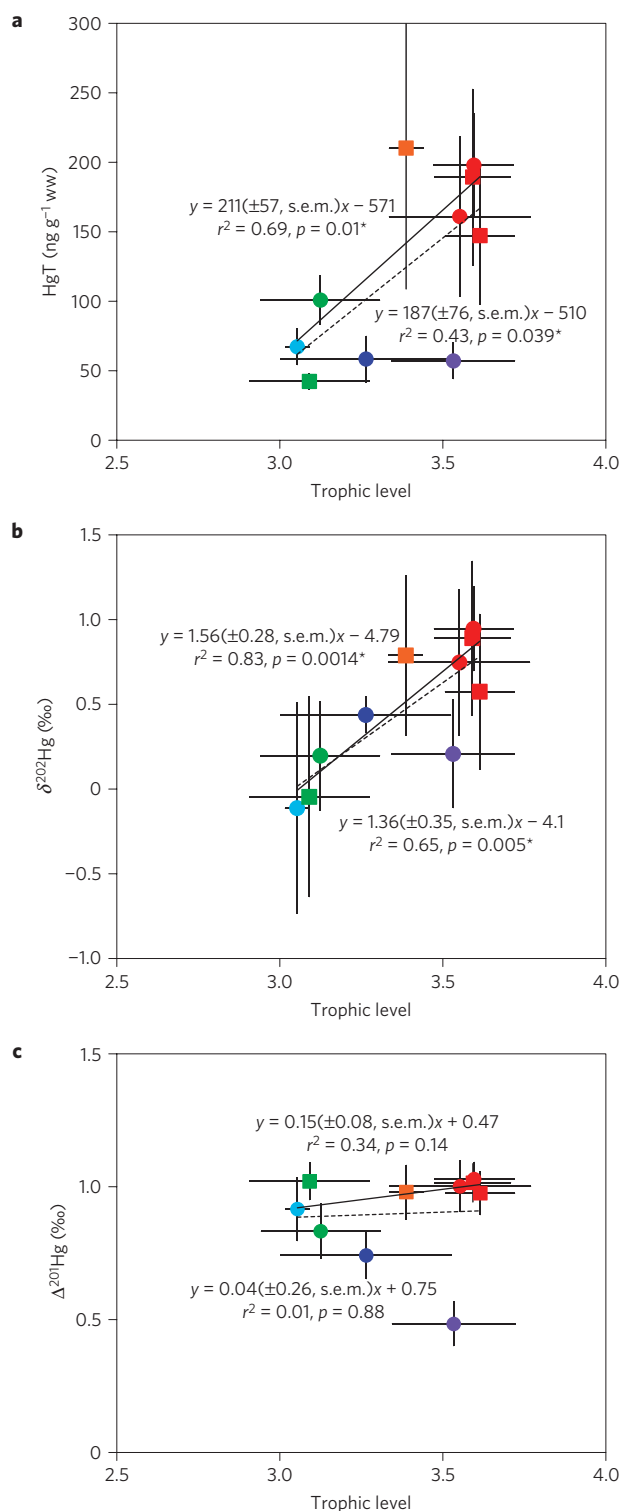


**Figure 3 | Ecological effects on mercury MDF and MIF in murre eggs.**

**a–c**, Influence of trophic levels (colony mean  $\pm \sigma$ , s.d.) on Hg concentrations (colony mean  $\pm \sigma$ , s.d.) (**a**), Hg MDF ( $\delta^{202}\text{Hg}$ , colony mean  $\pm \sigma$ , s.d.) (**b**) and Hg MIF ( $\Delta^{201}\text{Hg}$ , colony mean  $\pm \sigma$ , s.d.) (**c**) for murre egg sampling events (see Supplementary Table S1 for details and Fig. 1 for legend). The trophic levels of the eggs were estimated from  $\delta^{15}\text{N}$  measurements made on the samples using the method reported by Hobson and co-workers<sup>39</sup> and corrected for  $\delta^{15}\text{N}$  baseline shifts (see Supplementary Method S1). Solid lines show the regression trends for the southern Bering Sea and Gulf of Alaska eggs, and dashed lines show the regression trends for all colonies.

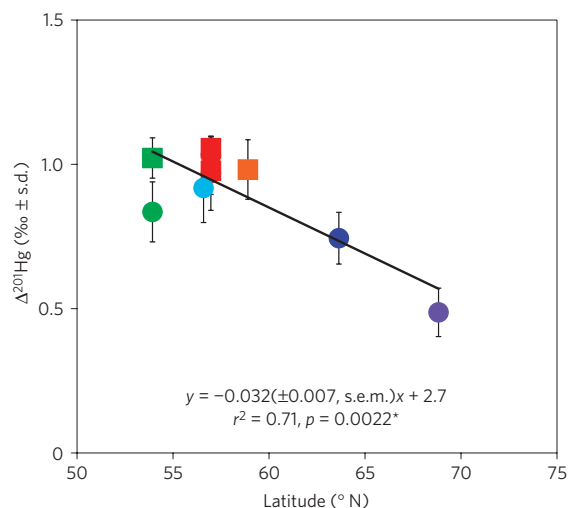


**Figure 4 | Effect of latitude on mercury MIF.** Colony mean  $\Delta^{201}\text{Hg}$  ( $\pm \sigma$ , s.d.) for common and thick-billed murre eggs collected at different latitudes in the Gulf of Alaska and Bering and Chukchi seas (see Fig. 1 for legend).

Climatic factors that may potentially influence aquatic Hg photochemistry across the latitudinal gradient are radiation fluxes and ice cover. Solar radiation fluxes differ partly because of geography and local climate in the western Gulf of Alaska (annual average  $111 \text{ W m}^{-2}$ ), Bering Sea ( $122 \text{ W m}^{-2}$ ) and eastern Chukchi Sea ( $104 \text{ W m}^{-2}$ ; ref. 44). Expressing egg Hg MIF against the radiation flux for the different colonies does not show a consistent trend, whether using radiation flux estimates expressed on an annual basis or on a seasonal basis covering April–June (arrival at breeding grounds until most eggs were laid, see Supplementary Fig. S4). This indicates that solar radiation fluxes might not be the dominant cause of the Hg MIF latitudinal trend. Large amounts of ice are still present in the Chukchi and northern Bering seas when murre arrive and begin occupying their nesting colonies (Fig. 1), and average egg Hg MIF values are correlated with the ice cover (expressed on a % concentration, Fig. 5). Sea ice is a proven barrier to Hg exchanges between the oceanic and the atmospheric reservoirs<sup>45</sup>. We therefore propose that the continuous decrease in egg MeHg MIF with increasing latitude predominantly reflects the negative feedback of sea-ice concentration on net photochemical degradation of MeHg.

### Hg Mass-independent fractionation and photochemistry

The relative magnitude of  $\Delta^{199}\text{Hg}$  and  $\Delta^{201}\text{Hg}$  anomalies may identify the different MIF mechanisms involved<sup>14</sup>. Experimental aquatic iHg and MeHg photoreduction produced  $\Delta^{199/201}\text{Hg}$  slopes of 1.00 and 1.36, respectively<sup>18</sup>. The agreement between this experiment and recently reviewed iHg and MeHg MIF anomalies in natural samples that define  $\Delta^{199/201}\text{Hg}$  slopes of  $1.03 \pm 0.03$  (s.e.m.) and  $1.30 \pm 0.02$  (s.e.m.), respectively<sup>14</sup>, indicates that Hg photochemistry may be the primary source of these anomalies in the environment. Although complementary iHg photoreduction experiments have shown a possible  $\Delta^{199/201}\text{Hg}$  slope variation, we assume iHg photoreduction in the natural environment generally follows the observed  $\Delta^{199/201}\text{Hg}$  reference slope of 1.03 (ref. 14). Freshwater and marine fish MeHg contents with  $\Delta^{199/201}\text{Hg}$  of 1.30 are therefore thought to originate from aquatic MeHg that has been partly photodegraded<sup>14,18,40</sup>. This  $\Delta^{199/201}\text{Hg}$  signature is then preserved in the food chain when MeHg is assimilated by primary producers and biomagnified up the food chain. Figure 6 shows that  $\Delta^{201}\text{Hg}$  and  $\Delta^{199}\text{Hg}$  for MeHg in murre eggs have a regression slope of 1.3 that indicates MeHg photodegradation to

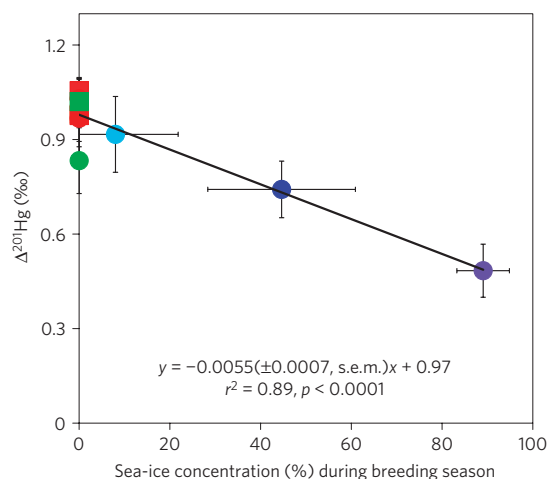


**Figure 5 | Influence of sea ice on egg mercury MIF.** Influence of 2002 sea-ice concentrations on Hg MIF  $\Delta^{201}\text{Hg}$  (colony mean  $\pm \sigma$ , s.d.) in common and thick-billed murre eggs (see Fig. 1 for legend). Seasonal ice concentration values represent the three-month mean condition ( $\pm \sigma$ , s.d.) from the arrival at the breeding grounds in early April until most eggs were laid in late June. Sea-ice values for the colonies integrate the 170 km foraging distance around the nesting locations (that is, the maximum foraging range shown by the dashed circles in Fig. 1a).

be the dominant MIF-inducing reaction regardless of the statistical method used (ordinary least squares:  $1.26\text{‰} \pm 0.06\text{‰}$  (s.e.m.); York regression, taking into account uncertainties in  $x$  and  $y$ :  $1.33\text{‰} \pm 0.06\text{‰}$  (s.e.m.)). Recent work on Hg MIF in Arctic snow driven by sunlight was shown to induce large negative snow  $\Delta^{199}\text{Hg}$  down to  $-5.3\text{‰}$  during an atmospheric mercury depletion event (AMDE) and subsequent photochemical Hg re-emission at Barrow (Chukchi Sea shore, Alaska, USA; ref. 46). On the assumption that this single AMDE event is representative of Arctic snow Hg photochemistry, and that murre eggs record a potential snowmelt Hg pulse, then seasonal sea-ice melting would potentially release Hg with highly negative  $\Delta^{199}\text{Hg}$  to the surface ocean. The  $\Delta^{199/201}\text{Hg}$  relation that accompanied snow Hg photoreduction was  $1.07 \pm 0.04\text{‰}$  (s.e.m.; ref. 46). On the basis of our observed murre egg MeHg  $\Delta^{199/201}\text{Hg}$  of 1.3, we suggest that net AMDE Hg deposition has not greatly impacted MeHg dynamics in the Alaskan marine system. Finally, post-emission transformations of Hg in the atmosphere may potentially induce MDF and MIF. Gratz and co-workers<sup>47</sup> observed positive Hg MIF in wet precipitation, with  $\Delta^{201}\text{Hg}$  ranging from  $+0.04$  to  $+0.52\text{‰}$ , and co-located vapour phase Hg with  $\Delta^{201}\text{Hg}$  of  $-0.16$  to  $+0.3\text{‰}$ . Although an exact oxidative or reductive atmospheric MIF mechanism could not be identified, the overall precipitation/vapour  $\Delta^{199/201}\text{Hg}$  of  $0.89 \pm 0.21\text{‰}$  (s.e.m.) is different from our observations.

### Anticipated effects of climate change on the Arctic Hg cycle

The magnitude of MeHg MIF in murre eggs can potentially be used as a proxy for sea-ice cover (see Supplementary Fig. S5). In addition, photochemical MeHg degradation can be quantified from the observed egg MeHg  $\Delta^{201}\text{Hg}$  and  $\Delta^{199}\text{Hg}$  by applying extrapolated MeHg photoreduction MIF fractionation factors to marine MeHg/DOC ratios (see Supplementary Method S2). Translating latitudinal MeHg MIF variations into MeHg photodegradation results in an approximate degradation increase from 8% to 16% when moving from the 90% ice-covered Cape Lisburne colony towards the 0% ice-covered Gulf of Alaska colonies. This indicates that the anticipated disappearance of Arctic sea ice in the twenty-first century might lead to a net increase in photochemical MeHg degradation by  $\sim 8\%$  (with an associated 50%

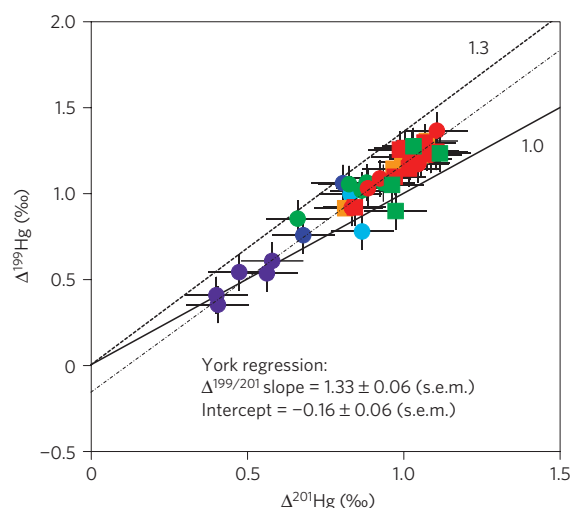


**Figure 6 | Odd-isotope anomalies in  $\Delta^{201}\text{Hg}$  versus  $\Delta^{199}\text{Hg}$  space.** The solid and dashed lines show the  $\Delta^{199/201}\text{Hg}$  slopes associated with natural iHg and MeHg photoreduction respectively, based on experiments<sup>18</sup> and a literature survey<sup>14</sup> (see Fig. 1 for legend). The dash-dot line represents the York regression trend for all samples. The uncertainties reported for the samples are the external reproducibility ( $n = 7$ ) of the method used for NIST Murre Egg Control Material QC04-ERM1 ( $\pm 0.11\text{‰}$ ,  $2\sigma$ , s.d. for  $\Delta^{199}\text{Hg}$ , and  $\pm 0.10\text{‰}$ ,  $2\sigma$ , s.d. for  $\Delta^{201}\text{Hg}$ ; see Supplementary Table S2b).

uncertainty, see Supplementary Method S2). In other words, an additional 4%–12% of the bioavailable marine MeHg pool might photodegrade in the absence of sea ice. Although this potential outcome is only a preliminary finding, it can still be used to estimate a first order of magnitude effect of climate change on a key abiotic process in the Arctic Hg cycle.

Our suggestion that marine MeHg MIF varies with ice cover provides the basis for using Hg MIF as a tracer for both ice cover and surface ocean photochemistry, and this tracer can be used on both recent and geological timescales. As the presence and melting of ice influences Arctic and sub-Arctic food web productivity, structure and species movements, warming in the Arctic will perturb ecosystems. As a result, MeHg MDF and MeHg MIF can be used to evaluate food web structures, and species movements and distribution in relation to ice cover, and this may prove to be a useful tool that can be used to help monitor changes in polar ecosystems in warming environments.

### Methods

**Sample collection.** Common and thick-billed murre (*U. aalge* and *U. lomvia*) eggs were collected from colonies in the Chukchi and Bering seas, and Gulf of Alaska during 1999–2002 (Fig. 1 and Supplementary Table S1). As noticeable temporal trends for Hg concentrations and isotopic compositions were not present in the St Lazaria eggs over the three sampling years, we pooled the data from this Gulf of Alaska nesting location. All of the egg samples were collected, processed and banked in the Marine Environmental Specimen Bank in Charleston, South Carolina, using previously described protocols and procedures<sup>18</sup>.

**Mercury concentrations.** Total Hg concentrations (based on wet mass) in egg contents were determined using isotope dilution cold vapour inductively coupled plasma mass spectrometry<sup>31</sup>. Accuracy was checked against NIST Standard Reference Material SRM 2976 (Mussel Tissue) and NIST QC04-ERM01 (Murre Egg Control Material), a perfect matrix-match in-house control material. No statistical differences were observed from the certificate values. Reproducibility was less than 0.6% difference for the NIST QC04-ERM01 replicates ( $n = 4$ ).

**Mercury stable isotope measurements.** Mercury isotopic compositions are expressed in  $\delta$  notation and reported in parts per thousands (‰) deviation from the NIST SRM 3133 standard, which was determined by sample–standard bracketing according to the following equation:

$$\delta^{xxx}\text{Hg}(\text{‰}) = [((^{xxx}\text{Hg}/^{198}\text{Hg})_{\text{Sample}} / (^{xxx}\text{Hg}/^{198}\text{Hg})_{\text{SRM3133}}) - 1] \times 1000$$

where  $xxx$  represents the mass of each mercury isotope between  $^{199}\text{Hg}$  and  $^{202}\text{Hg}$ . As a standard procedure<sup>35</sup>, we reported MDF with  $\delta^{202}\text{Hg}$ . MIF was reported using 'capital delta' notations ( $\Delta$ ) calculated as the difference between the measured  $^{xxx}\delta$  and the theoretically predicted  $^{xxx}\delta$  using MDF laws. Ranges below 10‰ were calculated using the following equations<sup>35</sup>:

$$\Delta^{199}\text{Hg}(\text{‰}) = \delta^{199}\text{Hg} - (\delta^{202}\text{Hg} \times 0.2520)$$

$$\Delta^{200}\text{Hg}(\text{‰}) = \delta^{200}\text{Hg} - (\delta^{202}\text{Hg} \times 0.5024)$$

$$\Delta^{201}\text{Hg}(\text{‰}) = \delta^{201}\text{Hg} - (\delta^{202}\text{Hg} \times 0.7520)$$

Mercury stable isotope measurements were made on a Neptune (Thermo) multiple collector inductively coupled plasma mass spectrometer (MC-ICPMS) at the Laboratoire des Mécanismes et Transferts en Géologie (Toulouse, France) equipped with a continuous-flow cold vapour generation system (Perkin Elmer FIAS-400 Hydride Generator). About 0.5 g of fresh-frozen egg homogenates was completely digested with 1.25 ml of a 4:1 (v/v) high-purity nitric acid/hydrogen peroxide mixture in Teflon-capped 35 ml glass digestion vessels placed in a closed high-pressure microwave system (CEM Discover; 190 °C, 280PSI, 15 min). Sample extracts diluted in 5% (v/v) nitric acid were mixed in the knotted reactor of the hydride generator with a 3% (w/v)  $\text{SnCl}_2/\text{HCl}$  reductant solution at flow rates of 0.5 ml  $\text{min}^{-1}$  and 0.3 ml  $\text{min}^{-1}$  respectively. Instrumental mass bias was corrected using a thallium internal standard (NIST SRM 977, 0.12 ml  $\text{min}^{-1}$ , Aridius II desolvating nebulizer), the exponential mass fractionation law and standard-sample-standard bracketing with NIST SRM 3133. All sample extracts matched the concentrations of the bracketing standards within 10%. Typical concentrations ranged between 0.5 and 2 ng  $\text{g}^{-1}$  (0.2 V–0.8 V) with acquisition times set to 15 min for sample series with Hg concentrations higher than 1 ng  $\text{g}^{-1}$  and 25 min for other sample series, leading to homogeneous counting statistics and precision across the concentration range. Typical blank values were negligible and below the detection limits of the instrument (<1–2 mV). Method performance was tested against a murre egg sample spiked with NIST SRM 3133, and no analytical and/or matrix artefacts were observed (see Supplementary Table S2a). Method accuracy was tested against an Almaden Hg standard distributed by the University of Michigan (J. D. Blum; see Supplementary Table S2b). Two biological reference materials, consisting of SRM 1947 (Lake Michigan Fish Tissue) and QC04-ERM1 (NIST Murre Egg Control Material), were analysed with reference values, and the associated uncertainties are reported in Supplementary Table S2b. As most of the egg samples cryogenically stored in the Marine Environmental Specimen Bank are available only in limited quantities, the samples were analysed only once, with the exception of the Murre Egg Control Material, QC04-ERM1, which had a reproducibility of  $\pm 0.26\text{‰}$  ( $2\sigma$ , s.d.,  $n = 7$ ) for  $\delta^{202}\text{Hg}$  and  $\Delta^{201}\text{Hg} \pm 0.10\text{‰}$  ( $2\sigma$ , s.d.,  $n = 7$ ) between batches throughout the course of the experiment.

**Nitrogen stable isotope measurements.**  $\delta^{15}\text{N}$  measurements were carried out after lipid removal by a continuous-flow isotope ratio mass spectrometer using methods published elsewhere<sup>39</sup>. Detailed information on method performance and the approach used to estimate the trophic levels of the seabirds after making corrections for the  $\delta^{15}\text{N}$  regional baseline shifts are presented in Supplementary Method S1 and Table S3.

**Satellite images.** The satellite images were obtained courtesy of the MODIS Rapid Response Project at NASA/GSFC.

**Sea-ice concentration data.** Sea-ice concentration data show the relative amounts of ice in 25 km by 25 km blocks. Concentrations are reported as per cents: 0% indicates ice is not present and 100% indicates complete cover. Data were obtained from SSM/I (ref. 49).

Received 27 September 2010; accepted 26 November 2010; published online 16 January 2011

## References

- Lindberg, S. *et al.* A synthesis of progress and uncertainties in attributing the sources of mercury in deposition. *Ambio* **36**, 19–32 (2007).
- Lockhart, W. L. *et al.* Concentrations of mercury in tissues of beluga whales (*Delphinapterus leucas*) from several communities in the Canadian Arctic from 1981 to 2002. *Sci. Total Environ.* **351**, 391–412 (2005).
- Braune, B. M. *et al.* Persistent organic pollutants and mercury in marine biota of the Canadian Arctic: An overview of spatial and temporal trends. *Sci. Total Environ.* **351**, 4–56 (2005).
- Campbell, L. M. *et al.* Mercury and other trace elements in a pelagic Arctic marine food web (Northwater Polynya, Baffin Bay). *Sci. Total Environ.* **351**, 247–263 (2005).
- Choi, A. L. & Grandjean, P. Methylmercury exposure and health effects in humans. *Environ. Chem.* **5**, 112–120 (2008).
- Schroeder, W. H. *et al.* Arctic springtime depletion of mercury. *Nature* **394**, 331–332 (1998).
- Outridge, P. M., Macdonald, R. W., Wang, F., Stern, G. A. & Dastoor, A. P. A mass balance inventory of mercury in the Arctic Ocean. *Environ. Chem.* **5**, 89–111 (2008).
- Ebinghaus, R. Mercury cycling in the Arctic—does enhanced deposition flux mean net-input? *Environ. Chem.* **5**, 87–88 (2008).
- St Louis, V. L. *et al.* Methylated mercury species in Canadian high arctic marine surface waters and snowpacks. *Environ. Sci. Technol.* **41**, 6433–6441 (2007).
- Cabana, G. & Rasmussen, J. B. Modelling food-chain structure and contaminant bioaccumulation using stable nitrogen isotopes. *Nature* **372**, 255–257 (1994).
- Loseto, L. L. *et al.* Linking mercury exposure to habitat and feeding behaviour in Beaufort Sea beluga whales. *J. Mar. Syst.* **74**, 1012–1024 (2008).
- Wilson, S. in *AMAP Workshop on Statistical Analysis of Temporal Trends of Mercury in Arctic Biota* (AMAP Report Vol. 3, AMAP, 2007).
- Macdonald, R. W., Harner, T. & Fyfe, J. Recent climate change in the Arctic and its impact on contaminant pathways and interpretation of temporal trend data. *Sci. Total Environ.* **342**, 5–86 (2005).
- Bergquist, R. A. & Blum, J. D. The odds and evens of mercury isotopes: Applications of mass-dependent and mass-independent isotope fractionation. *Elements* **5**, 353–357 (2009).
- Kritee, K., Barkay, T. & Blum, J. D. Mass dependent stable isotope fractionation of mercury during mer mediated microbial degradation of monomethylmercury. *Geochim. Cosmochim. Acta* **73**, 1285–1296 (2009).
- Zambardi, T., Sonke, J. E., Toutain, J. P., Sortino, F. & Shinohara, H. Mercury emissions and stable isotopic compositions at Vulcano Island (Italy). *Earth Planet. Sci. Lett.* **277**, 236–243 (2009).
- Laffont, L. *et al.* Anomalous mercury isotopic compositions of fish and human hair in the Bolivian Amazon. *Environ. Sci. Technol.* **43**, 8985–8990 (2009).
- Bergquist, B. A. & Blum, J. D. Mass-dependent and -independent fractionation of Hg isotopes by photoreduction in aquatic systems. *Science* **318**, 417–420 (2007).
- Buchachenko, A. L. *et al.* Magnetic isotope effect for mercury nuclei in photolysis of bis(p-trifluoromethylbenzyl)mercury. *Dokl. Phys. Chem.* **413**, 39–41 (2007).
- Thiemens, M. H. & Heidenreich, J. E. The mass-independent fractionation of oxygen—a novel isotope effect and its possible cosmochemical implications. *Science* **219**, 1073–1075 (1983).
- Farquhar, J., Bao, H. M. & Thiemens, M. Atmospheric influence of Earth's earliest sulphur cycle. *Science* **289**, 756–758 (2000).
- Jackson, T. A., Whittle, D. M., Evans, M. S. & Muir, D. C. G. Evidence for mass-independent and mass-dependent fractionation of the stable isotopes of mercury by natural processes in aquatic ecosystems. *Appl. Geochem.* **23**, 547–571 (2008).
- Das, R., Salters, V. J. M. & Odom, A. L. A case for in vivo mass-independent fractionation of mercury isotopes in fish. *Geochem. Geophys. Geosyst.* **10**, Q11012 (2009).
- Rodriguez-Gonzalez, P. *et al.* Species-specific stable isotope fractionation of mercury during Hg(II) methylation by an anaerobic Bacteria (*Desulfobulbus propionicus*) under dark conditions. *Environ. Sci. Technol.* **43**, 9183–9188 (2009).
- Kaufman, K. *Lives of North American Birds* (Houghton Mifflin Harcourt, 1996).
- Cramp, S. *Handbook of the Birds of Europe, the Middle East, and North Africa* (Oxford Univ. Press, 1985).
- Hatch, S. A., Meyers, P. M., Mulcahy, D. M. & Douglas, D. C. Seasonal movements and pelagic habitat use of murre and puffins determined by satellite telemetry. *Condor* **102**, 145–154 (2000).
- Ehrlich, P. R., Dobkin, D. S. & Wheye, D. *The Birder's Handbook: A Field Guide to the Natural History of North American Birds* (Simon & Schuster, 1988).
- Gaston, A. J. & Hipfner, J. M. in *The Birds of North America*, No. 497 (eds Poole, A. & Gill, F.) (The Birds of North America, 2000).
- Braune, B. M., Donaldson, G. M. & Hobson, K. A. Contaminant residues in seabird eggs from the Canadian Arctic. Part I. Temporal trends 1975–1998. *Environ. Pollut.* **114**, 39–54 (2001).
- Day, R. D. *et al.* Murre eggs (*Uriaaalgae* and *Urialomvia*) as indicators of mercury contamination in the Alaskan marine environment. *Environ. Sci. Technol.* **40**, 659–665 (2006).
- Programme-AMAP, AMAP Report. 2002.
- Davis, W. C. *et al.* An accurate and sensitive method for the determination of methylmercury in biological specimens using GC-ICP-MS with solid phase microextraction. *J. Anal. At. Spectrom.* **19**, 1546–1551 (2004).
- Furness, R. in *Birds as Monitors of Environmental Change* (eds Furness, R. & Greenwood, J. J. D.) 86–143 (Chapman & Hall, 1993).
- Blum, J. D. & Bergquist, B. A. Reporting of variations in the natural isotopic composition of mercury. *Anal. Bioanal. Chem.* **388**, 353–359 (2007).
- Ainley, D. G., Nettleship, D. N., Carter, H. R. & Storey, A. E. in *The Birds of North America Vol. 666* (eds Poole, A. & Gill, F.) 1–43 (Academy of Natural Sciences and American Ornithologists' Union, 2002).

37. Coyle, K. O., Hunt, G. L., Decker, M. B. & Weingartner, T. J. Murre foraging, epibenthic sound scattering and tidal advection over a shoal near St-George Island, Bering Sea. *Mar. Ecol.-Prog. Ser.* **83**, 1–14 (1992).
38. Springer, A. M., Roseneau, D. G., Murphy, E. C. & Springer, M. I. Environmental controls of marine food webs—food-habits of seabirds in the eastern Chukchi Sea. *Can. J. Fish. Aquat. Sci.* **41**, 1202–1215 (1984).
39. Hobson, K. A., Piatt, J. F. & Pitocchelli, J. Using stable isotopes to determine seabird trophic relationships. *J. Anim. Ecol.* **63**, 786–798 (1994).
40. Senn, D. B. *et al.* Stable isotope (N, C, Hg) study of methylmercury sources and trophic transfer in the Northern Gulf of Mexico. *Environ. Sci. Technol.* **44**, 1630–1637 (2010).
41. Jaffe, D. & Strode, S. Sources, fate and transport of atmospheric mercury from Asia. *Environ. Chem.* **5**, 121–126 (2008).
42. Sunderland, E. M. & Mason, R. P. Human impacts on open ocean mercury concentrations. *Glob. Biogeochem. Cycles* **21**, GB4022 (2007).
43. Biswas, A., Blum, J. D., Bergquist, B. A., Keeler, G. J. & Xie, Z. Q. Natural mercury isotope variation in coal deposits and organic soils. *Environ. Sci. Technol.* **42**, 8303–8309 (2008).
44. Dissing, D. & Wendler, G. Solar radiation climatology of Alaska. *Theor. Appl. Climatol.* **61**, 161–175 (1998).
45. Andersson, M. E., Sommar, J., Gardfeldt, K. & Lindqvist, O. Enhanced concentrations of dissolved gaseous mercury in the surface waters of the Arctic Ocean. *Mar. Chem.* **110**, 190–194 (2008).
46. Sherman, L. S. *et al.* Mass-independent fractionation of mercury isotopes in Arctic snow driven by sunlight. *Nature Geosci.* **3**, 173–177 (2010).
47. Gratz, L. E., Keeler, G. J., Blum, J. D. & Sherman, L. S. Isotopic composition and fractionation of mercury in Great Lakes precipitation and ambient air. *Environ. Sci. Technol.* **44**, 7764–7770 (2010).
48. Vander Pol, S. S. *et al.* Development of a murre (*Uria* spp.) egg control material. *Anal. Bioanal. Chem.* **387**, 2357–2363 (2007).
49. Nolin, A. R., Armstrong, R. L. & Maslanik, J. *Near-Real-Time SSM/I-SSMIS EASE-Grid Daily Global Ice Concentration and Snow Extent, (March–June 2002)*. National Snow and Ice Data Center (ed. Digital media, 1998) (updated daily).

## Acknowledgements

The samples used in this study were obtained from the Marine Environmental Specimen Bank (MESB) through the Seabird Tissue Archival and Monitoring Project (STAMP), a long-term collaborative effort by the Alaska Maritime National Wildlife Refuge (AMNWR), the National Institute of Standards and Technology (NIST), the US Geological Survey Biological Resources Division (USGS-BRD) and the Bureau of Indian Affairs Alaska Region Subsistence Branch (BLA-ARSB). We thank AMNWR and University of Alaska—Fairbanks (UAF) biologists, members of the St George Traditional Council, the Native Village of Point Hope IRA Council and residents of St George, Savoonga and Point Hope for collecting the eggs. We also thank K. S. Simac (USGS-BRD) for processing the eggs, M. B. Ellisor (NIST) for cryohomogenizing and banking the eggs and F. Poitrasson and Y. Godderis for providing helpful comments on the manuscript. This work is part of International Polar Year (IPY) Research Activity No. 439 ‘MERSAM’ (MERCURY Seabird Arctic Monitoring). Financial support for this research was provided by NIST, the French Centre National de la Recherche Scientifique, and Research Grant ANR-09-JCJC-0035-01 from the French Agence Nationale de Recherche.

## Author contributions

P.R.B., O.F.X.D., D.P. and R.D.D. designed the study; D.G.R. obtained the scientific collecting permits, made arrangements to collect the eggs and coordinated field logistics; and S.S.V. managed sample processing and banking. A.J.M. and R.S.P. were responsible for specimen processing, cryogenic banking and cryogenic homogenizations. Mercury isotopes were measured by D.P., R.D.D. and J.E.S. R.D.D. measured total mercury and K.H.H. measured nitrogen stable isotopes. D.P. and J.E.S. prepared the manuscript and all of the authors reviewed it.

## Additional information

The authors declare no competing financial interests. Supplementary information accompanies this paper on [www.nature.com/naturegeoscience](http://www.nature.com/naturegeoscience). Reprints and permissions information is available online at <http://npg.nature.com/reprintsandpermissions>. Correspondence and requests for materials should be addressed to D.P.